IDŐJÁRÁS

Quarterly Journal of the Hungarian Meteorological Service
Vol. 114, No. 4, October–December 2010, pp. 287–302

Modeling of the urban heat island pattern based on the relationship between surface and air temperatures

J. Unger[1*], T. Gál[1], J. Rakonczai[2], L. Mucsi[2], J. Szatmári[2], Z. Tobak[2], B. van Leeuwen[2], and **K. Fiala[3]**

[1]*Department of Climatology and Landscape Ecology, University of Szeged, P.O. Box 653, H-6701 Szeged, Hungary; E-mail: unger@geo.u-szeged.hu*

[2]*Department of Physical Geography and Geoinformatics, University of Szeged, P.O. Box 653, H-6701 Szeged, Hungary*

[3]*Directorate for Environmental Protection and Water Management of Lower Tisza District, P.O. Box 390, H-6701 Szeged, Hungary*

[*]*Corresponding author*

(Manuscript received in final form July 27, 2009)

Abstract—The aim of this study is to develop a new – and easy to use – method for early night-time near-surface air temperature pattern estimation based on surface temperature data in urban areas. The surface temperature data have been collected by an airborne thermal infrared sensor at an altitude of 2000 m above ground level. The study area was covered by hundreds of images with a spatial resolution of about 2 m. The measured values were calibrated with data of in situ surface measurements of different land use types. Simultaneous air temperature measurements were carried out using a car-based temperature sensor along an almost 12 km long N-S urban transect. The measured points were located using a GPS device. Data were processed with GIS methods, including newly developed algorithms. In order to find the relationship between air and surface temperatures a wider environment, the source area which determines the air temperature at a given point and time was taken into account. Using a source area with a radius of 500 m, a strong relationship was detected between the two parameters. Namely, the temperatures of the surfaces found in the surroundings (weighted by the distance) determine the temperature of the air parcel located at a given point. The obtained regression equation was applied to extend our results in order to model the air temperature field in a larger urban area.

Key-words: urban environment, surface and air temperatures, remote sensing, source area, Szeged, Hungary

1. Introduction

The thermal features of settlements are different from their natural surroundings. This phenomenon is related to the alteration of the original surface (material, geometry) and the by-products of human activity (heat, water vapor, pollution). As a consequence, a temperature excess develops in our living space in the near-surface air layer (compared to the rural areas). This is the so-called 'classical' *urban heat island* (UHI), already recognized at the end of the 18th century but named only much later by *Balchin* and *Pye* (1947).

As subsequent studies revealed, many kinds of UHIs can be defined. They include those defined according to the target medium (air, surface, sub-surface), the location (surface nature, height of measurement), and the type of sensor (*Roth et al*., 1989). Considering the thermal effect of cities according to these new approaches, they do not appear in an 'island' structure. Moreover, the investigations are often directed on the intra-urban variations of the temperature. Therefore, in these cases it is more appropriate to talk about the *urban temperature field* or *pattern*. Besides 'classical' UHI, this study concentrates on urban surface temperature patterns.

Cities present an almost limitless array of surface configurations (*Soux et al*., 2004). The detemination of the surface temperature in cities is difficult because of the complex structure of the urban-atmosphere interface (*Voogt* and *Oke*, 1997). In large urban areas it is usually measured indirectly by remote sensing technology mounted on satellite or aircraft platforms, but the sensor can be carried by car or manually too. In this case the problem is that the camera does not 'see' the total active surface because of the obstructions present on the 3D surface (*Roth et al*., 1989; *Soux et al*., 2004).

The temperature of the air (T_a) among the buildings is affected by the temperatures (T_s) of both horizontal and vertical surfaces (e.g., roofs, roads, tree tops, ground, walls) (*Voogt* and *Oke*, 1998). This multiple impact and the magnitudes of the effects of individual factors are very difficult to determine. *Voogt* and *Oke* (1997) introduced the concept of *complete surface temperature* which cannot be measured directly, but it can be calculated or estimated as a result of the radiation originating from all of the (horizontal and vertical) surfaces. Since such a detailed survey is extremely time-consuming, it cannot be applied in a larger area.

Roth et al. (1989) came up with the question of what the relationship is between surface and air temperature patterns. It is known that the nocturnal intra-urban variability in T_s is much smaller than the diurnal variability, while the opposite is true for T_a. As the near-surface climates are directly connected to the active surface (if the larger scale weather situation is favorable) there seems to be a contradiction. According to *Roth et al*. (1989), this could be due to the following: (i) lack of simple connection between the T_s and T_a values (implied also by *Goldreich* (1985)), (ii) remote sensors do not perceive the full active

surface, (iii) failure to recognize the different scales of climatic phenomena in the urban environment.

In the frame of a small review, we only go through the results of some earlier studies, which partly dealt with $T_s - T_a$ relationship. Because of the better geometric resolution, in these studies the surface infrared images were taken from airborne platforms (with one exception). The T_a data were obtained by mobile transects or fixed stations at 1.5–2 m above the ground. The observations of both parameters were taken at 'ideal' (calm and clear) weather conditions in the evening or at night. The parameters of the mentioned studies are summarized in *Table 1*.

Table 1. Parameters of nocturnal surface and air temperature measurements of some earlier studies

City	Thermo camera platform, altitude of flying	Pixel size	Type of stations	Source
Johannesburg	Aircraft, 400 m	2.5 m^2	Mobile	*Goldreich* (1985)
Malmö	Aircraft, -	1 × 2 m	Mobile	*Bärring et al.* (1985)
Göteborg	Aircraft, 600 m	2 × 2 m	Fixed, mobile	*Eliasson* (1992)
Göteborg	Manual	-	Fixed, mobile	*Eliasson* (1996)
Tel-Aviv	Helicopter, 2300 m	2 × 2 m	Mobile	*Ben-Dor* and *Saaroni* (1997)
Tel-Aviv	Helicopter, 2300 m	2 × 2 m	Mobile	*Saaroni et al.* (2000)

The investigation made by *Goldreich* (1985) is among the first of our subject. Results of both measurement methods indicate one nocturnal UHI core and a strong temperature gradient at about 600 m from the core, so the two temperature patterns overlap.

Bärring et al. (1985) found that high T_s can also be observed in suburban streets, provided that the streets are narrow enough. In contrast, T_a values decrease from the city center to the outskirts. According to their explanation, the air temperature is influenced both by the local street surface temperature, which is regulated by street geometry, and by the general thermal level of the surrounding city area determined by its general geometry and other UHI generating factors (air pollution, anthropogenic heat release).

Eliasson (1992) compared the two temperatures measured along a route in streets and squares in a central urban area. While she observed 5 ºC differences on the surface, the T_a variation was well-balanced with a range of only a few tenths of degrees. Later *Eliasson* (1996) draws attention to the fact that many studies do not make a clear distinction between surface and air temperatures. For example, the results of models predicting T_s are often compared or validated with field studies of T_a. She compared the variations in the two parameters along urban transects and found that the intra-urban surface and air temperature patterns are very different. T_s is influenced by the immediate urban structure (geometry), while T_a is not, so the former shows far larger fluctuations than the latter.

Ben-Dor and *Saaroni* (1997) compared surface and air temperature patterns measured separately along four N-S transects in a large urban area. The T_s values were computed as averages of about 40 pixel values around the spots of the T_a recordings. On and over uniform (asphalt) surfaces, they found strong relationships between the two temperature variations for all transects. *Saaroni et al.* (2000) generated isotherm maps from the measured T_s and T_a values along the four transects mentioned above. The obtained temperature fields were similar both in areal structure and magnitude.

The results of the mentioned studies are a bit contradictory. As *Voogt* and *Oke* (2003) summarized, the relations between the two parameters remained empirical and no simple general relation was found, but the correlations improved at night when microscale advection is reduced. It is clear that the complex interrelations between the two parameters in urban environments are not unambiguously detected or it is not even possible to describe them. Within this system, our research is focused on the area of impact which has an influence on the temperature of the near-surface air, presuming that a statistically based relationship can be established between the two temperatures if the size of this area is appropriately selected. Accordingly, the area of impact or *source area* is the place where the total impact of the physical features of its elements and their responses to the outer effects (heating-cooling, generation of turbulent processes) determine the temperature of a given air parcel.

The aim of this study is (i) to compare the air and surface temperatures developing in a complex urban environment, (ii) to reveal the relationship between them applying different source areas, and (iii) to generate an air temperature field for a large urban area with the help of the obtained relationship for two summer evenings, when the weather conditions in the preceding 36 hours were favorable for the microclimate modifying effects of the surface features.

2. Study area, weather situations

2.1. Szeged

Szeged is located in the southeastern part of Hungary (46°N, 20°E) at 79 m above sea level on a flat plain (*Fig. 1*). It belongs to the climatic region *Cf* according to Köppen's classification (temperate warm climate with uniform annual distribution of precipitation) (*Péczely*, 1979). Szeged provides a favorable background for urban climatological research, since its climate is free from the influences of orography and large water bodies, while its weather is characterized with high sunshine duration, low wind speed, and low precipitation (*Table* 2). Therefore, research on urban heat island and its consequences in Szeged has a several year long history (e.g., *Unger*, 1996; *Unger et al.*, 2001; *Kristóf et al.*, 2006).

Fig. 1. (a) City center, (b) housing estates, (c) detached houses with gardens, (d) industry and warehousing, (e) agricultural, green, and open area as land use types in Szeged.

The city's population of about 160,000 lives within an administration district of 281 km^2, but the highly urbanized area is restricted to an area of about 30–35 km^2. In the course of the 19th century, a structure of boulevards and avenues was established using the river Tisza as an axis. A large number of different land-use types are present including a densely built center with medium-wide streets and large housing estates of tall apartment buildings set in wide green spaces. There are zones used for industry and warehousing, areas occupied by detached houses, and considerable open spaces along the banks of the river, in parks, and around the city's outskirts (*Fig. 1*).

Table 2. Climate averages (1961–1990) in Szeged region (*WMO*, 1996)

Parameter	**August**	**Year**
Sunshine duration (h)	266	2023
Wind speed (m s^{-1})	2.8	3.4
Air temperature (°C)	20.2	10.5
Relative humidity (%)	69	75
Precipitation (mm)	57	495

2.2. Weather situations before and during the measurements

The observed T_a and T_s values depend not only on the momentary weather conditions but on the conditions prevailing in the previous (a few hours or days) time period as well. Therefore, a short description is given about the weather features of the 36-hour periods preceding the measurements of August 12 and 14, 2008 (between 18:30 and 19:30 UTC, see Section 3.1.).

The observations of the University station located at the edge of the city center were used to characterize the weather in the mentioned time period. Among them, the data of global radiation (G) and wind speed (v) are the most important, because these values reflect whether the weather was clear and calm (*Fig. 2*). According to the data, the insolation was undisturbed during the daylight hours (regular bell-shape G variation) with maximum values of 810 – 860 W m^{-2}. On the whole, the air movement was moderate (0 – 4.7 m s^{-1}) and during the measurements, it ranged between 0.8 and 3.1 m s^{-1}. Since the wind speed was measured at 26 m above ground level, it was likely to be significantly smaller at the street level. The days were rather warm with maximum values of 28 –36 ºC and with minimum values of 17–22 ºC at dawn.

Consequently, during the investigated period, the weather conditions promoted the microclimatic effects of the surface features in Szeged.

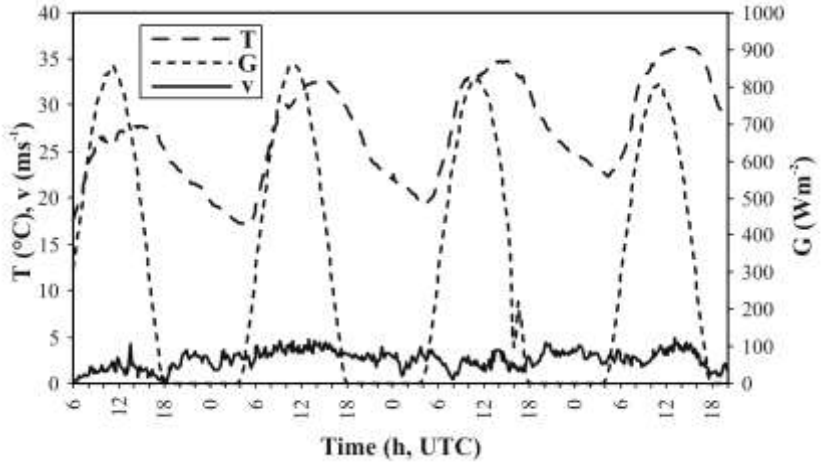

Fig. 2. Variation of global radiation (G), air temperature (T), and wind speed (v) at the University station during the measurements and the preceding one and a half days (06:00 UTC, August 11, 2008 − 20:00 UTC, August 14, 2008).

3. Methods

3.1. Temperature measurements

The measurements in August took place in the 1.5 –2-hour periods immediately after sunset, because there was no direct shortwave radiation disturbing the signals recorded by the camera at that time and the flight did not violate the flight ban

after 22:00 LST. As sunset was at 19:57 LST (17:57 UTC), the airborne images were taken between 18:15 and 19:45 UTC, the surface and near-surface measurements were performed between 18:30 and 19:30 UTC. Thus, 19:00 UTC (1 hour after sunset) can be regarded as a reference time of all measurements. It is worth to note that test measurements were taken on July 29, 2008 in order to optimize the flying parameters, spots, and route of the surface and near-surface observations, as well as to harmonize the work of the different measurement teams (flying – 3, mobile measurement – 2, measurements by hand – 4 people).

3.1.1. Mobile air temperature measurements along a N-S urban transect

Mobile measurements are widespread in studying urban climatic parameters (e.g., *Conrads* and *van der Hage*, 1971; *Eliasson*, 1996; *Voogt* and *Oke*, 1997; *Henninger* and *Kuttler*, 2007). In our case the temperature observations were carried out by an automatic radiation-shielded sensor (DCP D100089 HiTemp) connected to a digital data logger (LogIT DataMeter 1000) that provided data at every 2 seconds. In order to diminish the thermic disturbing effect of the car, the sensor was located on a bar 0.6 m before the car and 1.45 m above the ground. Due to the requirements of efficient ventilation and data density, the speed of the car was 20–25 km h^{-1}, and thus the data were gathered every 11–14 m. The locations of the data along the measurement route were recorded by GPS. Data measured at the compulsory stops (red light, barrier etc.) were later deleted from the database.

The 11.8 km long measurement route is a N-S transect of Szeged crossing the typical urbanized land use areas of the city (housing estates, detached houses with gardens, city center, industry, and warehousing). One-hour measurements were taken there and back along the route in order to make time adjustments to the reference time (19:00 UTC) assuming linear air temperature change with time at this period of the day (*Oke* and *Maxwell*, 1975). This linear change was also observed in the records of the University weather station (*Fig. 2*). In order to get uniform temperature distribution along the route, the route was divided by 15 m, then the averages of the mean values of the readings taken separately there and back on the 15 m long sections were computed (*Fig. 3*). Thus, there are altogether $2 \times 786 = 1572$ T_a values, which refer to the middle points of these sections.

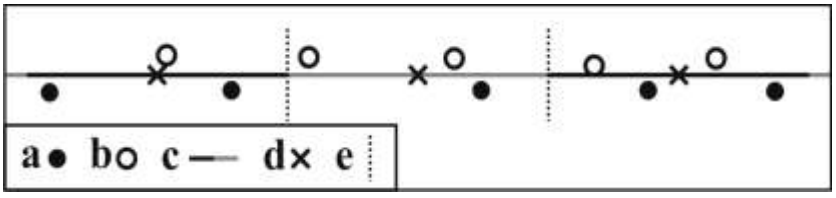

Fig. 3. An example on the spots of air temperature values regarded at the averaging route. (a) spots there, (b) spots back, (c) 15 m long sections, (d) section centers, (e) section borders.

The relative temperatures by points along the route (that is the UHI intensity) were determined by regarding the value of the minimum T_a as a UHI intensity of 0 ºC.

3.1.2. Surface temperature measurements in the urban environment using an airborne thermal camera

The thermal measurements were carried out using a self-developed low-cost small-format digital imaging system. The current system is based on the experiences gained during earlier research using thermal (*Mucsi et al.*, 2004) and CIR (color-infrared) small format aerial photography (SFAP) data collected with a small airplane (*Rakonczai et al.*, 2003; *Szatmári et al.*, 2008). The system is based on a FLIR ThermaCam P65 thermal camera integrated with a navigation system and a GPS/GNSS receiver (Mobile Mapper CE).

The FLIR (forward looking infrared radiometer) is a compact single-band thermal camera with a temperature sensitivity of 0.08 °C. The instrument can measure temperatures between −40 °C and +500 °C and has a resolution of 320×240 pixels. The camera has germanium lenses to register the thermal radiation emitted by the object of investigation.

The flight plan determined the data collection density during the survey. Since a fixed photographic lens was used for the camera, the flying speed, height, and the distance between consecutive flight lines defined the overlap between adjacent images. For later post-processing purposes, an overlap of at least 20–30% was needed. To collect data at the required density, one image per 4 seconds was recorded while flying with a speed of 120 km h^{-1} at a height of 2000 m.

Before the flight, a detailed flight plan (*Fig. 4*) was created, and during the survey this plan was followed as accurately as possible. A Mobile Mapper CE GPS/GNSS receiver provided navigational aid during the flight and recorded the actual high precision GPS flight track, which was used for positioning the images during the post-processing phase.

After the survey, the acquired data needed to be post-processed. Using software specifically designed for the analysis of the thermal images, several parameters needed to be readjusted. Using the results of the fieldwork carried out at the same time as the flight, the data was inspected and calibrated (see Section 3.1.3.). The temperature data collected by the thermal camera was refined based on the time-synchronized field measurements of the same evening as the flight. After this, the thermographic data was stored in a file as a matrix, containing the calibrated temperatures.

The next step in the thermal processing chain was the extraction of the coordinates and time data from the GPS track log recorded during the flight. This data was connected to the camera log file that stores the precise time of every recorded image. With this operation, EOV coordinates were generated for

every image center. During the next step, the center coordinate and the image resolution were combined to create a so-called world file. A world file is a simple text file that was used to georeference the thermal images. Using this georeference, a first, coarse geometric correction was executed with an accuracy of about 100–150 meter, depending on the weather circumstances during the flight (*Fig. 5*). In the next step, the images were combined to one single image, resulting in a thermal mosaic with a spatial resolution of 2.5 m, covering the complete survey area (*Fig. 6*).

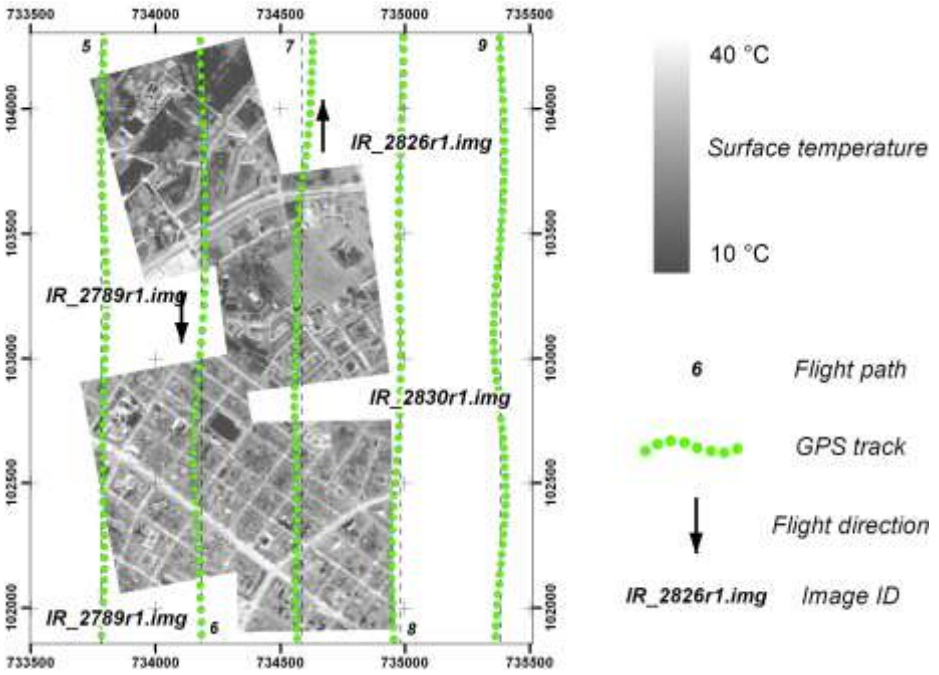

Fig. 4. Flight plan with real GPS track and calibrated sample thermal images of the city.

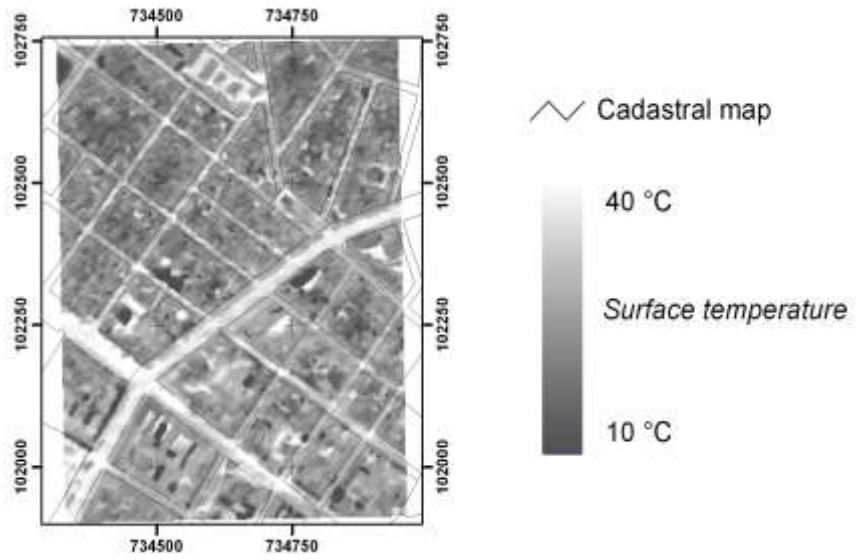

Fig. 5. Georeferenced (Hungarian EOV) thermal image with cadastral vector layer.

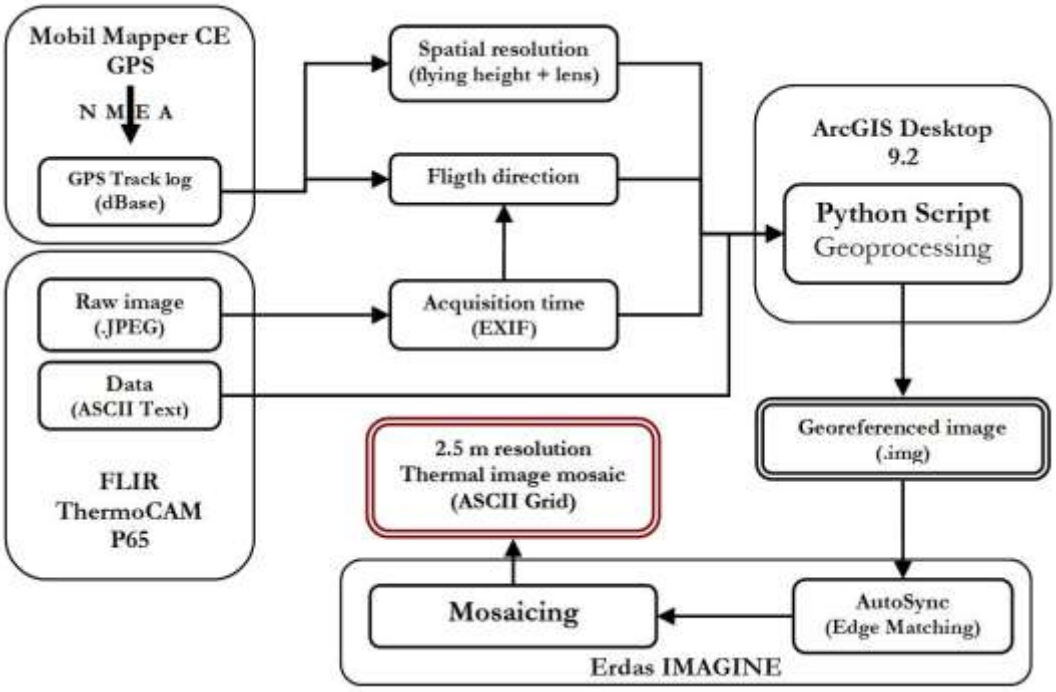

Fig. 6. Flowchart of the image processing.

It was assumed that some decrease can be found in the surface temperatures during the flight times (50 and 51 minutes on August 12 and 14, respectively). If this dependence from the time is significant, the pixel values have to be corrected to the middle time (19:00 UTC) of the survey according to the general cooling tendency. A statistically established trend was found only in the evening of August 14 (*Fig. 7*).

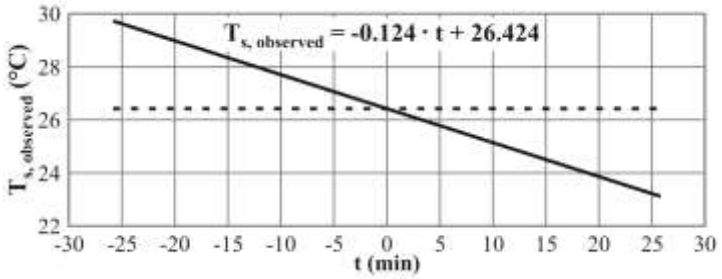

Fig. 7. Regression line of the pixel values ($T_{s,observed}$) as a function of time (t) in August 14, 2008.

In order to refer the pixel values to the middle time, these values were corrected by the obtained cooling rate: the values before the middle time were lowered; the ones after the middle time were increased:

$$T_{s,observed} = -at + b, \qquad T_s = T_{s,observed} + at,$$

where $T_{s,observed}$ is the measured pixel value, a is the slope of the regression line,

t is the time in minutes (–25.5 − 25.5), b is the value of the regression line at the middle time, and T_s is the corrected pixel value. Henceforth T_s means the uncorrected and corrected surface temperature in August 12 and 14, respectively.

3.1.3. In situ surface temperature measurements in selected points of representative urban surfaces

The temperature of the surface was measured directly by hand (DCP D100047 ProTemp sensor, LogIT DataMeter 1000 data logger) in the 40 selected points representing the urban surfaces in two sample areas (*Fig. 1*). These T_s values are necessary for the calibration of the airborne thermal images, namely for transforming the relative temperature scale of the images to an absolute scale.

3.2. Statistical method to reveal the relationship between air and surface temperatures

As mentioned in Section 1, the air temperature at a given point at 1.5 m above ground level depends not only on the immediate surface under it and its own temperature. The T_a of this point is a result of the total effects of the turbulent heat transports generated by the surrounding heated surfaces. Several studies looking for T_a−T_s relationship point out the importance of the micro-advection in the near-surface air layer (e.g., *Roth et al.*, 1989), which promotes the mixing of the thermal properties in a wider environment. Therefore, to investigate this connection a larger area, the source area and its thermal features have to be taken into account. According to the related literature, this source area covers an area with a radius of a few hundred meters around the measurement point, and in the case of calm weather it can be regarded as a circle. In case of a temperature sensor at 1.5–2 m above ground level in urban environment, the circle has a radius of maximum 0.5 km, but this is likely to depend on the building density (*Oke*, 2004).

These active surfaces are not only horizontal but also vertical (e.g., walls). In affecting the value of T_a, the role of the surfaces nearer to the point is more important compared to the ones farther away. It has to be taken into account that in the case of 1.5 m level, the role of the roofs is likely to be smaller than the role of the ground surfaces (pavements, roads, parking lots, grass areas, etc.). In our case, only the temperatures of the horizontal surfaces can be detected on the thermal images, thus we can only use these temperatures in searching for the relationship between T_a and T_s.

For the determination of the size of the source area for the T_a values along the transect and the distance-based weighting of the pixel values inside it, different approaches were applied. Only those are presented here which gave the best results in investigating the relationship and that are in accordance with the conditions mentioned above.

Among the results of the manual T_s measurements, the lowest value was 19.4 ºC, however, the possibility of lower values occurring in the investigated area cannot be excluded. After the air temperature data was processed, it became clear that there are areas detected by the camera that have temperatures that are up to 15 degrees lower than the directly surrounding surface. The reason for this is the heterogeneity of the urban environment. The camera was setup to use normal calibration values. The physical properties of the roofs constructed from metal considerably differ from the standard calibration values. Highly reflective surfaces like aluminum, copper, or stainless steel work as a mirror resulting in false temperature measurements. The false temperatures were identified and filtered out of the images.

As a second step, according to the maximum size of the source area mentioned above (*Oke*, 2004), circles with a radius r (r = 100–500 m) around the points of T_a values were selected (see Section 3.1.1.). The (filtered) T_s pixel values of these circles were taken by weighting, the farthest (r) values with a factor of 0.5, the nearest ones (0 m) with a factor of 1, and the ones between them with a proportionality factor between 0.5 and 1. Thus, the weighted and averaged surface temperature ($T_s(wr)$) regarding a given point's surrounding with a radius of r is determined by the next formula:

$$T_S(wr) = \frac{\sum_{i=1}^{n} T_{Si} \cdot \left(1 - \frac{D_i}{2r}\right)}{\sum_{i=1}^{n} \left(1 - \frac{D_i}{2r}\right)}, \quad (1)$$

where T_{Si} is the ith pixel value, D_i is the distance of the ith pixel from the given point, and the summation refers to all (not filtered) pixels inside the circle with a radius of r. In order to automate this calculation for all points along the transect, an algorithm was developed in the ArcView Avenue script language.

4. Results

Fig. 8 shows the variations of the UHI intensity along the transect on the two evenings. The reference place (with the lowest T_a value) is located in an area with abundant vegetation almost at the south end of the transect. In cities in the temperate climate zone during 'ideal' weather conditions the maximum development of the UHI occurs 3–5 hours after sunset because of the different cooling rates of urban and rural areas (*Oke*, 1987). Therefore, in our case (1 hour after sunset), the obtained UHI intensities are likely to be smaller than the maximum values occurring during the same night.

In the evening of August 12 the intensity was relatively high (~2 ºC) at the north end of the transect, wich can be attributed to the area characterized with buildings of a housing estate. Going towards the south, two maximums

reaching almost 3 ºC occurred: the first one in an area with large artificial surfaces (shopping centers, parking lots), while the second one appeared in the densely built-up city center. From here the intensity decreases almost continuously towards the south end of the transect.

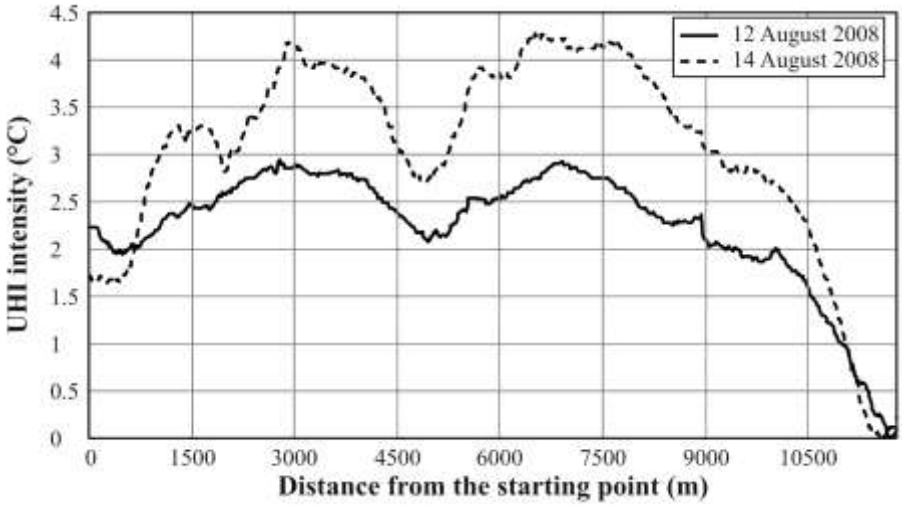

Fig. 8. UHI intensities along the N-S transect in Szeged (19:00 UTC, August 12 and 14, 2008), starting point at the north.

On August 14, the variation of the intensity was very similar to the previous one with the exceptions of the maximum values, which exceeded even 4 ºC this evening.

Since the measurement route was located inside the urban area, the obtained intensity values reflect the intra-urban temperature variation rather than the real magnitude of the UHI. Namely, when we talk about the heat island, the urban temperatures are usually compared to the temperatures of the surrounding rural ('natural') areas (*Oke*, 1987; *Lowry*, 1977). This can also be an explanation for the moderate magnitude of the obtained maximum UHI values in this study.

According to the method described in Section 3.2, several relationships can be obtained between the T_a values along the transect and the $T_s(wr)$ values computed by Eq. (1) with different radii (two measurements − n = 1572). As *Table 3* shows, the relationships are significant in all cases (even at a level of 0.1% at this high number of element pairs), however, the larger the radius the stronger the connection between the two parameters (to the upper limit of *r*, see Section 3.2.). This can be explained by the thermal compensatory effect of the larger area and confirm the possible size of the source area related to the air temperature measured at a level of 1.5 m in urban environments. Since the best relationship is derived in the case of $r = 500$ m, henceforth the regression equation obtained in this case is applied to extend our results: to model the spatial distribution of T_a in a larger urban area in the case of the investigated two evenings.

Table 3. Relationships between T_s and T_a along the urban transect and their parameters regarding the surroundings with different radius r (R^2 is the determination coefficient, R is the correlation coefficient, σ_R is the standard deviation around the regression line) on August 12 and 14, 2008 (n = 1572)

r (m)	Regression equation	R^2	R	σ_R	Significance level
100	$T_a = 0.373 \times T_s(w100) + 17.691$	0.574	0.757	0.858	< 0.001
200	$T_a = 0.406 \times T_s(w200) + 16.898$	0.611	0.781	0.820	< 0.001
300	$T_a = 0.426 \times T_s(w300) + 16.453$	0.642	0.801	0.787	< 0.001
400	$T_a = 0.436 \times T_s(w400) + 16.228$	0.663	0.814	0.763	< 0.001
500	$T_a = 0.447 \times T_s(w500) + 15.982$	0.685	0.828	0.738	< 0.001

In the course of the extension of our results, surface temperatures in the whole study area were used as input data in a 100 m × 100 m mesh for modeling the air temperature fields in the evenings of August 12 and 14. Since for computing $T_s(w500)$ the pixel values around the mesh points ($r = 500$ m) are needed, the modeling area is smaller (~ 21 km^2) compared to the originally recorded area (marked by intermittent line in *Fig. 1*). The deficiencies at the corners are caused by some errors in the flying paths.

The modeled air temperature field on August 12 has large areas with a temperature greater than 26.5 ºC. This area is located in the city center and streches out towards NW, where industrial and warehousing land use dominates (*Fig. 9a*). A temperature extension is present in NE direction, where the large housing estates can be found. The cooler areas of the low built-up districts, the outer green zones, and the belt of the Tisza River and its banks (at NW, SW, and SE) are also recognizable. On the whole, a difference of about 3 ºC occurs in the area which is in accordance with the temperature range experienced along the transect in this evening (*Figs. 8* and *9a*).

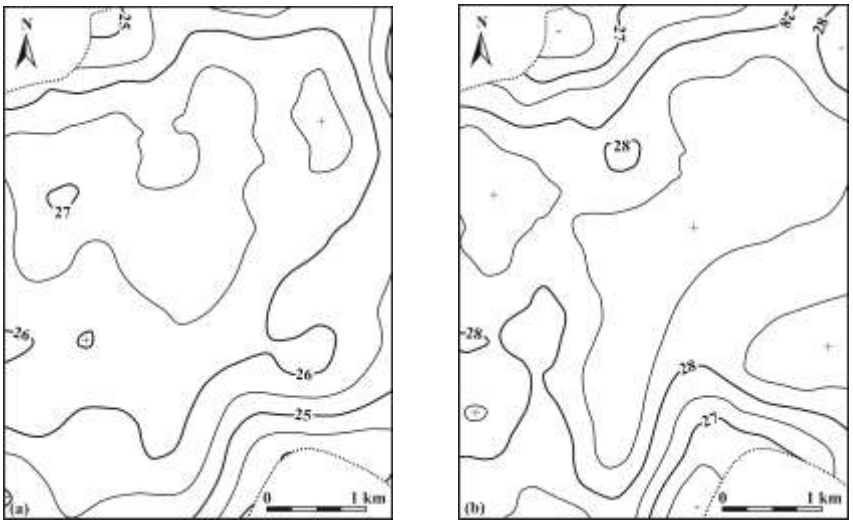

Fig. 9. Modeled air temperature patterns in Szeged at 19:00 UTC, (a) August 12 and (b) August 14, 2008 (location of the area is shown in *Fig. 1*).

The values of the modeled air temperature pattern on August 14 are higher than the values of the previous one (*Fig. 9b*). As on August 12, basically the warmest (> 28.5 ºC) areas can be found in the center, in the NW and NE parts, augmented towards the south. Broadly speaking, the cooler areas are also the same. On the whole, also a difference of about 3 ºC occurs in the area, which is a bit lower than the temperature range measured along the transect of this evening (*Figs. 8* and *9b*).

5. Conclusions

In this study we tried to reveal a statistical (but physically supported) connection between the air and surface temperatures measured in an urban environment. During the data collection, airborne and surface-based remote sensing (indirect) and traditional (direct) tools and methods were applied. In order to search for the mentioned relationship, a wider environment, the source area was taken into account, which determines the air temperature at a given point and time. As the results show, using a source area with a radius of 500 m, a strong relationship was detected between the two parameters. Namely, the temperatures of the surfaces found in the surroundings (weighted with the distance) decisively influence the temperature of the air parcel located at a given point. The obtained regression equation was applied to extend our results in order to model the air temperature field in a larger urban area in the investigated two evenings.

By all means we should not forget that the obtained relationship is based on the data of only two, however complex, measurement campaigns. In the future, when using data of more measurements on days with similar environmental conditions to that of the investigated days, the result could be refined. Based on these new results we can make steps to the generalization of the operation mechanisms between the urban air and surface temperatures. In the frame of this study, a data collection in different seasons could also be a new direction, which can provide a possibility to examine the specific seasonal features and enable their comparison.

***Acknowledgements*—**This work was supported by the Hungarian Scientific Research Fund (OTKA T048400, K-67626). The authors' special thanks are due to *G. Barna, K. Balogh, N. Kántor, Z. Ladányi, Z. Sümeghy, T. Unger* taking part in the measurements and to *E. Tanács* for the language revision of the manuscript.

References

Balchin, W.G.V. and *Pye, N.,* 1947: A micro-meteorological investigation of Bath and the surrounding district. *Q. J. Roy. Meteor. Soc. 73,* 297-319.

Bärring, L., Mattsson, J.O. and *Lindqvist, S.,* 1985: Canyon geometry, street temperatures and urban heat island in Malmö, Sweden. *J. Climatol. 5,* 433-444.

Ben-Dor, E. and *Saaroni, H.*, 1997: Airborne video thermal radiometry as a tool for monitoring microscale structures of the urban heat island. *Int. J. Remote Sens. 18*, 3039-3053.

Conrads, L.A. and *van der Hage, J.C.H.*, 1971: A new method of air-temperature measurement in urban climatological studies. *Atmos. Environ. 5*, 629-635.

Eliasson, I,, 1992: Infrared termography and urban temperature patterns. *Int. J. Remote Sens. 13*, 869-879.

Eliasson, I., 1996: Urban nocturnal temperatures, street geometry and land use. *Atmos. Environ. 30*, 379-392.

Goldreich, Y., 1985: The structure of the ground heat island in a central business district. *J. Clim. Appl. Meteorol. 24*, 1237-1244.

Henninger, S. and *Kuttler, W.*, 2007: Methodology for mobile measurements of carbon dioxide within the urban canopy layer. *Climate Res. 34*, 161-167.

Kristóf, G., Bányai, T. and *Rácz, N.*, 2006: Development of computational model for urban heat island convection using general purpose CFD solver. *Preprints 6th Int Conf on Urban Climate*, Göteborg, Sweden, 822-825.

Lowry, W.P., 1977: Empirical estimation of urban effects on climate: A problem analysis. *J. Appl. Meteorol. 16*, 129-135.

Mucsi, L., Kiss, R., Szatmári, J., Bódis, K., Kántor, Z., Dabis, G. and *Dzsupin, M.*, 2004: The analysis of contamination deriving from the leakage of subsurface pipeline networks via remote sensing (in Hungarian). *Geodézia és Kartográfia 56*/4, 3-8.

Oke, T.R., 1987: *Boundary Layer Climates.* 2nd edition. Routledge, London-New York.

Oke, T.R., 2004: Siting and exposure of meteorological instruments at urban sites. *27th NATO/CCMS Int Tech Meeting on Air Pollution Modelling and Application*. Kluwer, Banff, Canada, 14 p.

Oke, T.R. and *Maxwell, G.B.*, 1975: Urban heat island dinamics in Montreal and Vancouver. *Atmos. Environ. 9*, 191-200.

Péczely, G., 1979: *Climatology* (in Hungarian). Tankönyvkiadó, Budapest.

Rakonczai, J, Csató, Sz, Mucsi, L, Kovác,s F, Szatmári, J, 2003: Experiences on the evaluation of the 1999 and 2000 excess waters (in Hungarian). *Vízügyi Közlemények Különszám IV,* 317-336.

Roth, M., Oke, T.R. and *Emery, W.J.*, 1989: Satellite-derived urban heat islands from three coastal cities and the utilization of such data in urban climatology. *Int. J. Remote Sens. 10*, 1699-1720.

Saaroni, H., Ben-Dor, E., Bitan, A. and *Potchter, O.*, 2000: Spatial distribution and microscale characteristics of the urban heat island in Tel-Aviv, Israel. *Landscape Urban Plan 48*, 1-18.

Soux, A., Voogt, J.A. and *Oke, T.R.*, 2004: A model to calculate what a remote sensor 'sees' of an urban surface. *Bound.-Lay. Meteorol. 111*, 109-132.

Szatmári, J., Tobak, Z., van Leeuwen, B., Olasz, A. and *Dolleschall, J.*, 2008: An effective and low-cost method to detect environmental contaminations: the promise of CIR small format aerial photography. *12th Geomathematics Conf.*, Mórahalom, Hungary.

Unger, J., 1996: Heat island intensity with different meteorological conditions in a medium-sized town: Szeged, Hungary. *Theor. Appl. Climatol. 54*, 147-151.

Unger, J., Sümeghy, Z. and *Zoboki, J.*, 2001: Temperature cross-section features in an urban area. *Atmos. Res. 58*, 117-127.

Voogt, J.A. and *Oke, T.R.*, 1997: Complete urban surface temperatures. *J. Appl. Meteorol. 36*, 1117-1132.

Voogt, J.A. and *Oke, T.R.*, 1998: Radiometric temperatures of urban canyon walls obtained from vehicle traverses. *Theor. Appl. Climatol. 60*, 199-217.

Voogt, J.A. and *Oke, T.R.*, 2003: Thermal remote sensing of urban climates. *Remote Sens. Environ. 86*, 370-384.

WMO, 1996: *Climatological normals (CLINO) for the period 1961-1990.* WMO/OMM-No. 847, Geneva.